DFT investigation of electronic structures and magnetic properties of halides family $MeHal_3$ (Me=Ti, Mo,Zr,Nb, Ru, Hal=Cl,Br,I) one dimensional structures.

A. A. Kuzubov[1], E. A. Kovaleva[1], M. I. Popova[1], A. S. Kholtobina[1], N. S. Mikhaleva, M. A. Visotin[2,1] ,A. S. Fedorov[2,1]

[1]Siberian Federal University, av. Svobodny 79, Krasnoyarsk, 660041, Russia

[2]Kirensky Institute of Physics, Akademgorodok 50, Krasnoyarsk, 660036, Russia

Keywords: transition metal trihalides, magnetic properties, thermoelectric conversion, density functional theory

[*]Corresponding author: alex99@iph.krasn.ru, phone: +07-904-8985175.

Abstract

Using DFT GGA calculations, electronic structure and magnetic properties of wide family of transition metal trihalides ($TMHal_3$) (Zr, Ti and Nb iodides, Mo, Ru, Ti and Zr bromides and Ti or Zr chlorides) are investigated. These structures consist of transition metal atoms chains surrounded by halides atoms. Chains are connected to each other by weak interactions. All $TMHal_3$ compounds were found to be conductive along chain axis except of $MoBr_3$ which is indirect gap semiconductor. It was shown that NbI_3 and $MoBr_3$ have large magnetic moments on metal atoms (1.17 and 1.81 μ_B, respectively) but other $TMHal_3$ materials have small or zero magnetic moments. For all structures ferromagnetic and anti-ferromagnetic phases have almost the same energies. The causes of these properties are debated.

1. Introduction

At present, as new nanostructure synthesis methods are developed, more and more attention is paid for synthesis and description of new one-dimensional structures properties. In practice, such nanostructure chains are often linked together by weak dispersive interactions. Thus, they may serve as a one-dimensional conductors or semiconductors that should lead to a strong anisotropy of their optical properties. Also such materials having semiconductor properties can be used in practice to create different optical elements: IR sensors, absorbing devices, etc.. Weak interactions between neighboring chains due to van der Waals forces should lead to softening of the phonon vibrations along the directions perpendicular to the chain axis and, consequently, to a decrease in the thermal conductivity λ along these directions. This can also be used in practice to create new thermoelectric converters (TC) [1], where the efficiency is defined by thermoelectric figure-of-merit, ZT [2], as a product of working temperature T, Seebeck coefficient squared S^2, electrical conductivity σ, divided by the thermal conductivity. Therefore “phonon engineering”, i.e creation of materials having low thermal conductivity due to structural fragment separation at the nanoscale is now represented as one of the most promising ways to create highly effective TC. Along with that, TC material is demanded to have large density of states near the Fermi level. This allows one to suppose that one-dimensional transition metal trihalides ($TMHal_3$) having weak van-der-Waals interaction between chains would show low heat conductance in the directions perpendicular to the chain axis and high density of states in the vicinity of Fermi level due to presence of metal atoms having d(f) electrons. It is assumed that these materials can serve as effective materials for TC construction.

Even though the family of $TMHal_3$ has been known for more than 50 years [3, 4], and their structure is well-investigated, there is only a few data available regarding physical properties of these compounds, particularly, electronic structure and magnetic properties [5]. Purpose of this work is to fill this gap. $TMHal_3$ family compounds can adopt various structures consisting of octahedra bonded to each other through the vertexes and forming chains in particular direction (ReO_3, RhF_3, $AlCl_3$, TiI_3-type structures). Amongst them, the TiI_3-type is somewhat outstanding in terms of having quasi-one-dimensional structure of these chains (see Figure 1). These unique compounds can be, in turn, distinguished into hexagonal TiI_3-type and orthorhombic $RuBr_3$-type.

It is known that temperature increasing up to 323 K may cause structural transition from hexagonal to orthorhombic crystal system in TiI_3 [6]. Semiconducting nature of some TiI_3-like structures was reported by Angelkort et al. [7]. In this paper, using quantum chemical calculations we examine the electronic structure and magnetic properties of a wide range of $TMHal_3$ compounds adopting quasi-one-dimensional structure, namely, Zr, Ti and Nb iodides, Mo, Ru, Ti and Zr bromides and Ti or Zr chlorides.

2. The calculations details.

All quantum chemical calculations were performed within the framework of density functional theory using plane wave basis set and projector augmented wave method [8,9] as implemented in Vienna Ab-initio Simulation Package [10–13]. GGA-PBE spin polarized exchange-correlation functional [14] and Grimme D3 [15] correction for van-der-Waals interactions were used for electronic and structural optimization in all cases. Residual forces acting on atoms being less than 10^{-3} eV/Å were used as stopping criteria for cell vectors and geometry optimization. Monkhorst-Pack k-point first Brilloin zone sampling [16] was used with k-point mesh containing 6x6x6 points along three translation vectors.

3. Results

First, unit cells of all mentioned above transition metal trihalides were optimized. Table 1S of Supplementary material summarizes data regarding unit cell parameters, space group and interatomic distances for the structures under investigation. All of these compounds adopt “chain” structure with chemically bonded atoms forming columns along the **c** translation vector.

Figure 1 shows two different crystal structures being realized in this type of compounds. Zirconium trihalides and ruthenium bromide were found to be diamagnetic while titanium, niobium and molybdenum compounds possess magnetic moment.

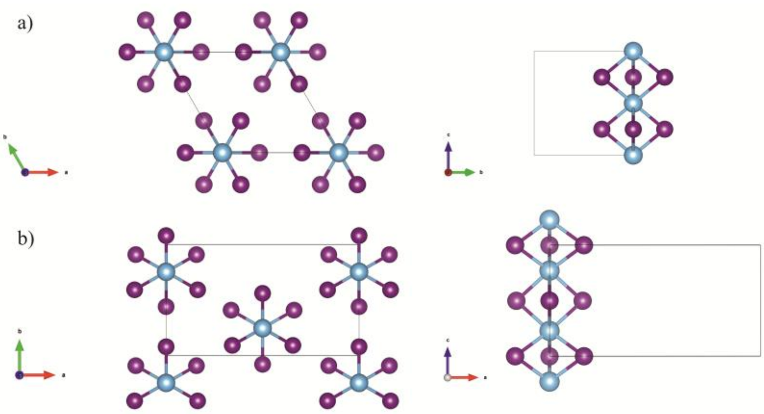

Figure 1. Unit cells for transition metal trihalides. a) hexagonal, b) orthorhombic structure

It was established that TM atoms antiferromagnetic ordering were more favorable than ferromagnetic one for all cases, see Table 1.

Table 1. Magnetic moment (*M*) on the TM atoms and energy difference $\Delta E = E_{ferro} - E_{antiferro}$ between ferro- and antiferromagnetic states.

Compound	M, $\mu_Б$	ΔE, eV
ZrI_3	0.000	–
TiI_3 (hex)	0.249	0.005
TiI_3	0.300	0.004
NbI_3	1.166	0.018
$MoBr_3$	1.805	0.053
$RuBr_3$	0.00	–
$TiBr_3$	0.129	0.001
$ZrBr_3$	0.000	–
$TiCl_3$	0.043	0.002
$ZrCl_3$	0.000	–

Analysis of spin density shows it is mainly located on TM atoms, and, depending on the nature of metal, unpaired electrons occupy different orbitals, see Figure 2. Small energy differences between ferro- and antiferromagnetic states (maximum value of 0.05 eV corresponds to $MoBr_3$) witness the weak exchange between TM d-orbitals where unpaired electrons are located.

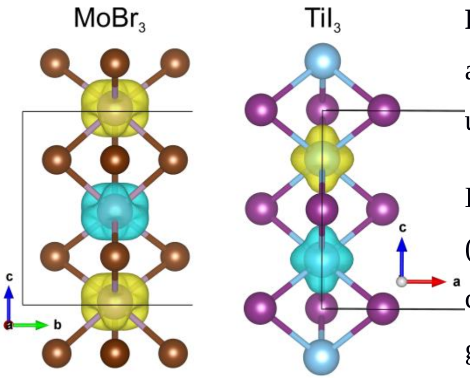

Figure 2. Characteristic of the spin density distribution in $MoBr_2$ and TiI_3 compounds. Yellow and blue areas correspond to spin - up and spin-down densities, respectively.

Band structure and density of state (DOS) calculations showed (see Figure 3, Figure 1S of Supplementary material) metallic conductivity in all compounds except of $MoBr_3$ which is indirect gap semiconductor with a gap of ~ 1.1 eV (Figure 3c). The most valuable contribution to the DOS nearby the Fermi level rises from TM d-electrons, see Figure 3 and Figure 1S.

Once TMH_3 compounds adopt "chain" structure along the c vector, the issue of nature of bonding between chains is fundamental. The analysis of TMH_3 band structures along the directions other than Γ–Z (corresponding to the chain axis) showed band dispersion suggesting chemical bonding between neighboring chains, in agreement with earlier tight-binding calculations [5]. Band structures of TiI_3(orth), TiI_3(hex), $TiBr_3$, $ZrBr_3$, $TiCl_3$, $ZrCl_3$ nearby the Fermi level is analogous to that of ZrI_3. Its main feature is significant band dispersion along Γ–Z direction and weak dispersion along perpendicular directions. Thus, a hole pocket will be formed along the Γ–Z direction causing hole type of conductivity in these systems. In order to elucidate its nature, spatial electron density distributions for the corresponding band was analyzed. According to the Figure 4, the band is formed by the interacting transition metal d_z^2-orbitals. This fact confirms the suggestion regarding weak exchange interaction formation through the direct exchange between transition metal d-orbitals. Overlapping area depends on the TM-TM distance and the size of d-orbitals which is changed according to the TM atom size belonging either to third or fourth rows. This, in turn, influences to the interaction energy. So, the size of the d-orbital plays a key role in the magnetic moments formation. d_z^2-orbitals of 3d Ti atoms are too small to overlap with each other which leads to the localization of d-electrons giving rise to magnetic moment whereas 4d elements have large orbitals with larger overlapping resulting in zero magnetic moment. Fermi level crossing bands of $RuBr_3$ are similar to ones described above but in directions other than Z–Γ these states are vacant witnessing electron type of conductivity. Bands formed by the d_z^2-orbitals of TM atoms are lower in energy for NbI_3 and $MoBr_3$ (see Figure 3b and 3c), thus being fully occupied and not contributing to magnetic moment of the system, see Fig 4d.

Figure 3. Band structure, total (DOS) and partial densities of states (POS) for antiferromagnetic ground state of (a) ZrI_3, (b) NbI_3; (c) $MoBr_3$, (d) $RuBr_3$. Red and blue lines correspond to the PDOS of metal and halogen atoms, respectively.

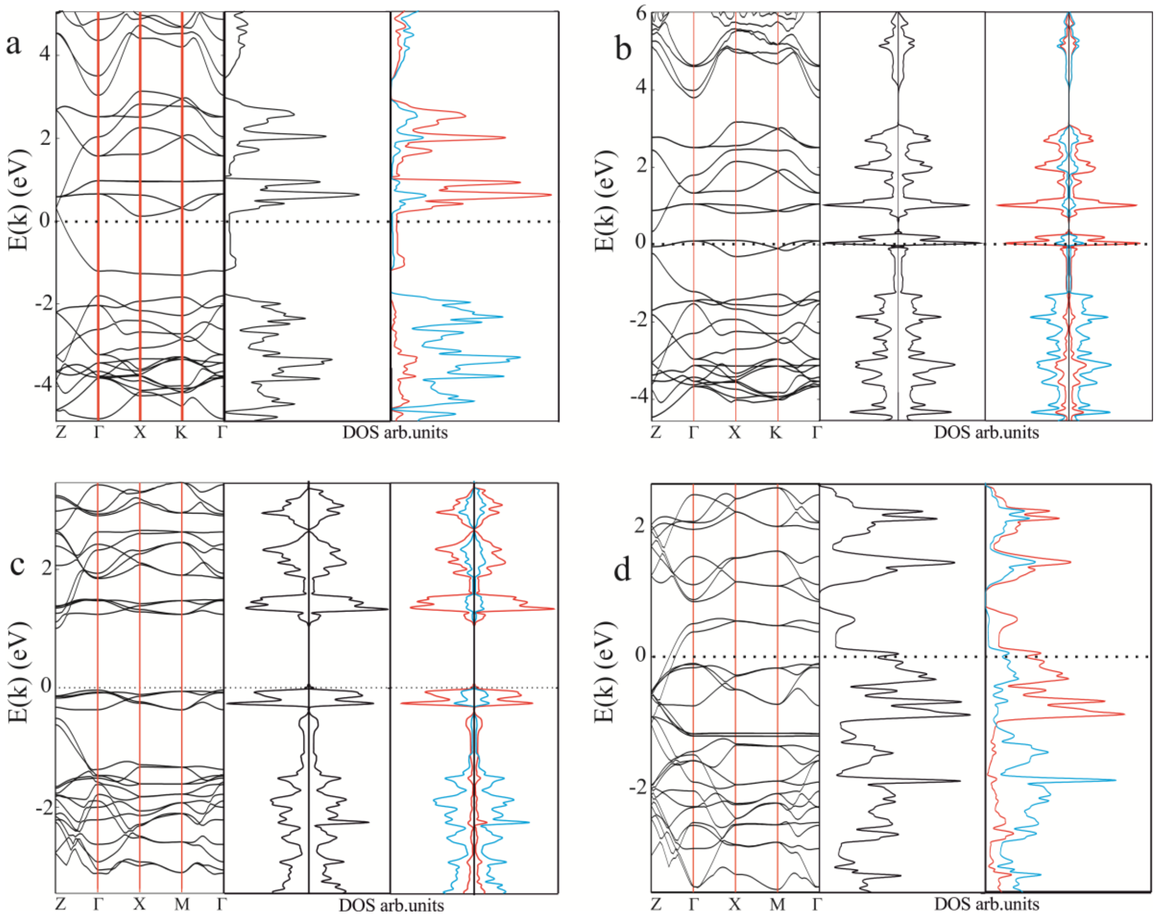

Weak band dispersion in the proximity of Fermi level in all directions is characteristic for NbI_3 and $MoBr_3$. Spatial electron density distribution analysis showed that TM half-occupied d-orbitals don't interact with each other being located distant from TM-Hal bonds, see Fig 4d.. This results in the localization of spin density (Figure 2) and magnetic moment increasing (see Table 1).

Figure 4. Electron density distribution for bands in the Fermi level vicinity for (a) ZrI_3; (b) TiI_3; (c) $RuBr_3$; (d) NbI_3.

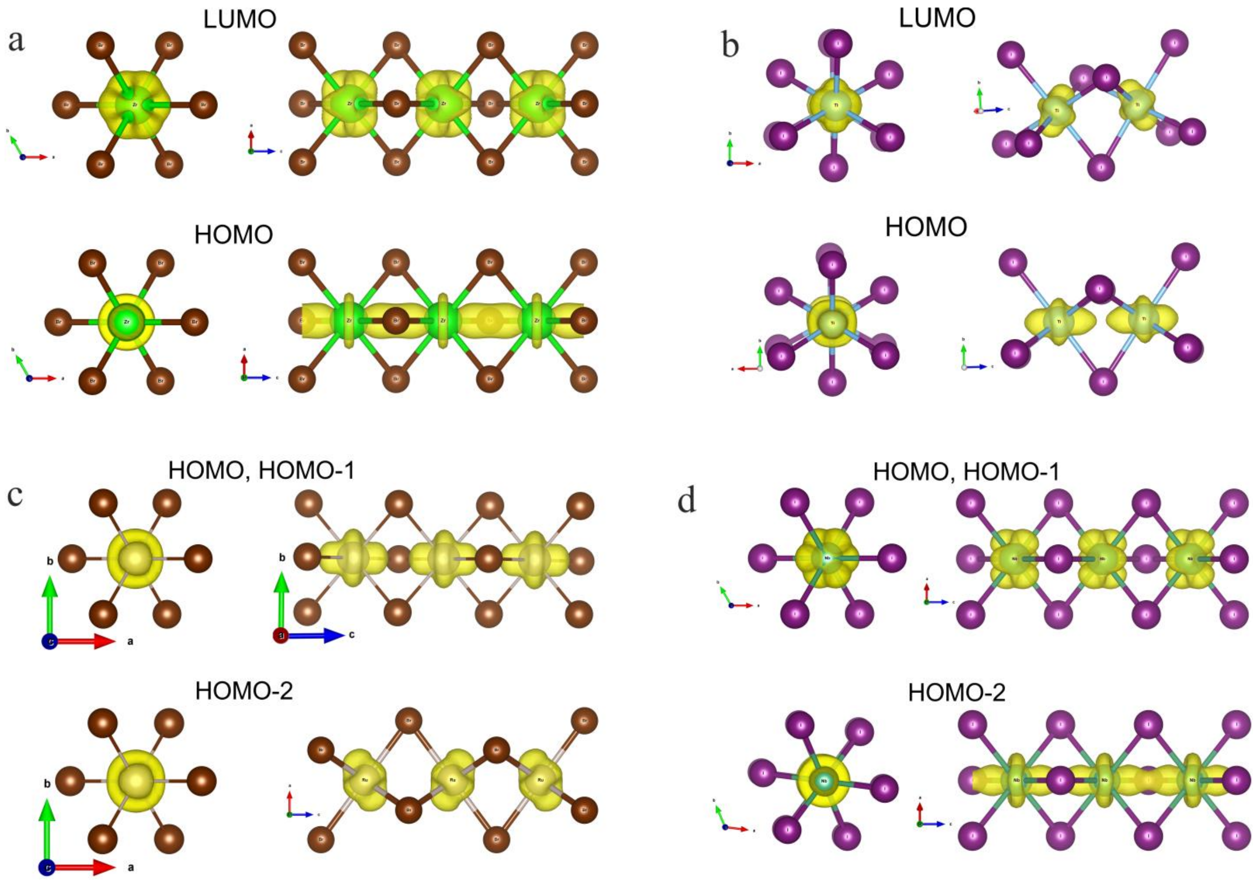

4. Conclusions

By DFT quantum chemical calculations the electronic structure and magnetic properties of the wide family of transition metal trihalides having chain structures are investigated. It is shown the origin of the large metal atom magnetic moments inside NbI_3 and $MoBr_3$ is strong localization of the metal d-orbitals, flat band structure and large density of states near the Fermi level. In other cases there is a substantial dispersion of electronic bands along the chain axis at the Fermi level which is the cause of conduction along the chain axis. In all cases the ferromagnetic and antiferromagnetic phases have almost the same energies because of weak overlapping of d-orbitals of the nearest transition metal atoms. It is assumed that TiI_3 , $TiCl_3$ and NbI_3 materials due to the high density of states near the Fermi level and weak interaction between chains can be promising materials for thermoelectric applications.

Acknowledgments

This work was supported by the Russian Science Foundation, project no. 16-13-00060. N.S.M. thanks the Russian Foundation for Basic Research, project RFBR 16-32-60003 mol_a_dk, for the financial support of ZrI_3, TiI_3 and NbI_3 electronic structure calculations.

References:

1. Rowe, D.M. Thermoelectric waste heat recovery as a renewable energy source / D.M. Rowe // Int. J. Innov. Energy Syst. Power. – 2006. – Vol. 1, № 1. – P. 13–23.

2. Faraji, Y. et al. Electric Power Generation using Thermoelectric Cells and Evacuated Tube Solar Collectors / Y. Faraji, A. Akbarzadeh, J. Leblanc, R. Singh, C. Bourke // Solar2010, 48th AuSES Annu. Conf. – 2010. – – P. 1–13.

3. Baker, W.A. et al. Magnetic properties of zirconium (III) and hafnium (III) iodides / W.A. Baker, A.R. Janus // J. Inorg. Nucl. Chem. – 1964. – Vol. 26, № 12. – P. 2087–2097. [doi:10.1016/0022-1902(64)80153-6]

4. Michel, C. et al. Structural relationships in compounds with R3c symmetry / C. Michel, J. M. Moreau, W.J. James // Acta Crystallogr., Sect. B. – 1971. – Vol. B27. - P 501. [doi:10.1107/S0567740871002437]

5. Lin, J. et al. Dimensional diversity in transition metal trihalides /J. Lin, G. J. Gordon // lnorg. Chem. – 1993. – Vol. 32. – P. 1476. [doi: 10.1021/ic00060a025]

6. Hillebrecht, H. et al. About Trihalides with TiI3 Chain Structure: Proof of Pair Forming of Cations in β-RuCl3 and RuBr3 by Temperature Dependent Single Crystal X-ray Analyses / H. Hillebrecht, T. Ludwig, G. Thiele // Zeitschrift für Anorg. und Allg. Chemie. – 2004. – Vol. 630, № 13–14. – P. 2199–2204. [doi:10.1002/zaac.200400106]

7. Angelkort, J. et al. Temperature-dependent neutron diffraction on TiI_3 / J. Angelkort, A. Senyshyn, A. Schönleber, S. van Smaalen // Zeitschrift für Krist. – 2011. – Vol. 226, № 8. – P. 640–645. [doi:10.1524/zkri.2011.1370]

8. Blöchl, P.E. Projector augmented-wave method / P.E. Blöchl // Phys. Rev. B. – 1994. – Vol. 50, № 24. – P. 17953–17979. [doi:10.1103/PhysRevB.50.17953]

9. Kresse, G. et al. From ultrasoft pseudopotentials to the projector augmented-wave method / G. Kresse, D. Joubert // Phys. Rev. B. – 1999. – Vol. 59, № 3. – P. 1758–1775. [doi:]10.1103/PhysRevB.59.1758

10. Kresse, G. et al. Efficient iterative schemes for *ab initio* total-energy calculations using a plane-wave basis set / G. Kresse, J. Furthmüller // Phys. Rev. B. – 1996. – Vol. 54, № 16. – P. 11169–11186. [doi:10.1103/PhysRevB.54.11169]

11. Kresse, G. et al. *Ab initio* molecular dynamics for liquid metals / G. Kresse, J. Hafner // Phys. Rev. B. – 1993. – Vol. 47, № 1. – P. 558–561. [doi:10.1103/PhysRevB.47.558]

12. Kresse, G. et al. *Ab initio* molecular-dynamics simulation of the liquid-metal–amorphous-semiconductor transition in germanium / G. Kresse, J. Hafner // Phys. Rev. B. – 1994. – Vol. 49, № 20. – P. 14251–14269. [doi:10.1103/PhysRevB.49.14251]

13. Kresse, G. et al. Efficiency of ab-initio total energy calculations for metals and semiconductors using a plane-wave basis set / G. Kresse, J. Furthmüller // Comput. Mater. Sci. – 1996. – Vol. 6, № 1. – P. 15–50. [doi:10.1016/0927-0256(96)00008-0]

14. Perdew, J.P. et al. Generalized Gradient Approximation Made Simple / J.P. Perdew, K. Burke, M. Ernzerhof // Phys. Rev. Lett. – 1996. – Vol. 77, № 18. – P. 3865–3868. [doi:10.1103/PhysRevLett.77.3865]

15. Grimme, S. et al. A consistent and accurate ab initio parametrization of density functional dispersion correction (DFT-D) for the 94 elements H-Pu / S. Grimme, J. Antony, S. Ehrlich, H. Krieg // J. Chem. Phys. – 2010. – Vol. 132, № 15. – P. 154104. [doi:10.1063/1.3382344]

16. Monkhorst, H.J. et al. Special points for Brillouin-zone integrations / H.J. Monkhorst, J.D. Pack // Phys. Rev. B. – 1976. – Vol. 13, № 12. – P. 5188–5192. [doi:10.1103/PhysRevB.13.5188]

17. Babel, D. Die Verfeinerung der MoBr3-Struktur / D. Babel // J. Solid State Chem. – 1972. – Vol. 4, № 3. – P. 410–416. [doi:10.1016/0022-4596(72)90156-9]

18. Merlino, S. et al. Order−Disorder Transformation in RuBr3 and MoBr3: A Two-Dimensional Ising Model / S. Merlino, Luca Labella, * and Fabio Marchetti, S. Toscani // – 2004. – Vol. 16, № 20. – P. 3895–3903. [doi:10.1021/cm049235q]

19. Natta, G. et al. The different crystalline modifications of TiCl3, a catalyst component for the polymerization of α-olefins. I: α-, β-, γ-TiCl3. II: δ-TiCl3 / G. Natta, P. Corradini, G. Allegra // J. Polym. Sci. – 1961. – Vol. 51, № 156. – P. 399–410. [doi:10.1002/pol.1961.1205115602]

Supplementary material

Table 1S. Calculated and published crystal structures, space groups and structural parameters of transition metal trihalides $TMHal_3$

Compound	Crystal structure	Space group	Cell parameters	Nearest TM-TM atoms distance, Å	Nearest H-H atoms distance, Å		
			a	b	c		
ZrI_3	Hexagonal	P63/mcm	7.25 [4]	7.25	6.64	3.32	4.18
			7.42	7.42	6.58		
TiI_3	Orthorhombic	Pmmn	12.27 [5]	7.09	6.48	2.96, 3.35	4.12
			12.94	7.01	6.42		
	Hexagonal	P63/mcm	7.14	7.14	6.51	3.26	4.17
			7.15	7.15	6.36		
NbI_3	Hexagonal	P63/mcm	6.61 [4]	6.61	6.82	3.34	4.20
			7.16	7.16	6.67		
$MoBr_3$	Orthorhombic	Pmmn	6.60 [15]	11.42	6.06	2.92, 3.14	3.91
			6.50	11.40	5.99		
$RuBr_3$	Orthorhombic	Pmmn	6.49 [16]	11.24	5.86	2.73	3.82
			6.26	11.13	5.90		
$TiBr_3$	Hexagonal	P63/mcm	6.60 [4]	6.60	6.10	3.05	3.89
			6.51	6.51	5.90		
$ZrBr_3$	Hexagonal	P63/mcm	6.73 [4]	6.73	6.30	3.15	3.98
			6.90	6.90	6.18		
$TiCl_3$	Hexagonal	P63/mcm	6.27 [17]	6.27	5.82	2.91	3.72
			6.10	6.10	5.63		
$ZrCl_3$	Hexagonal	P63/mcm	6.38 [4]	6.38	6.14	3.07	3.78
			6.45	6.45	6.01		

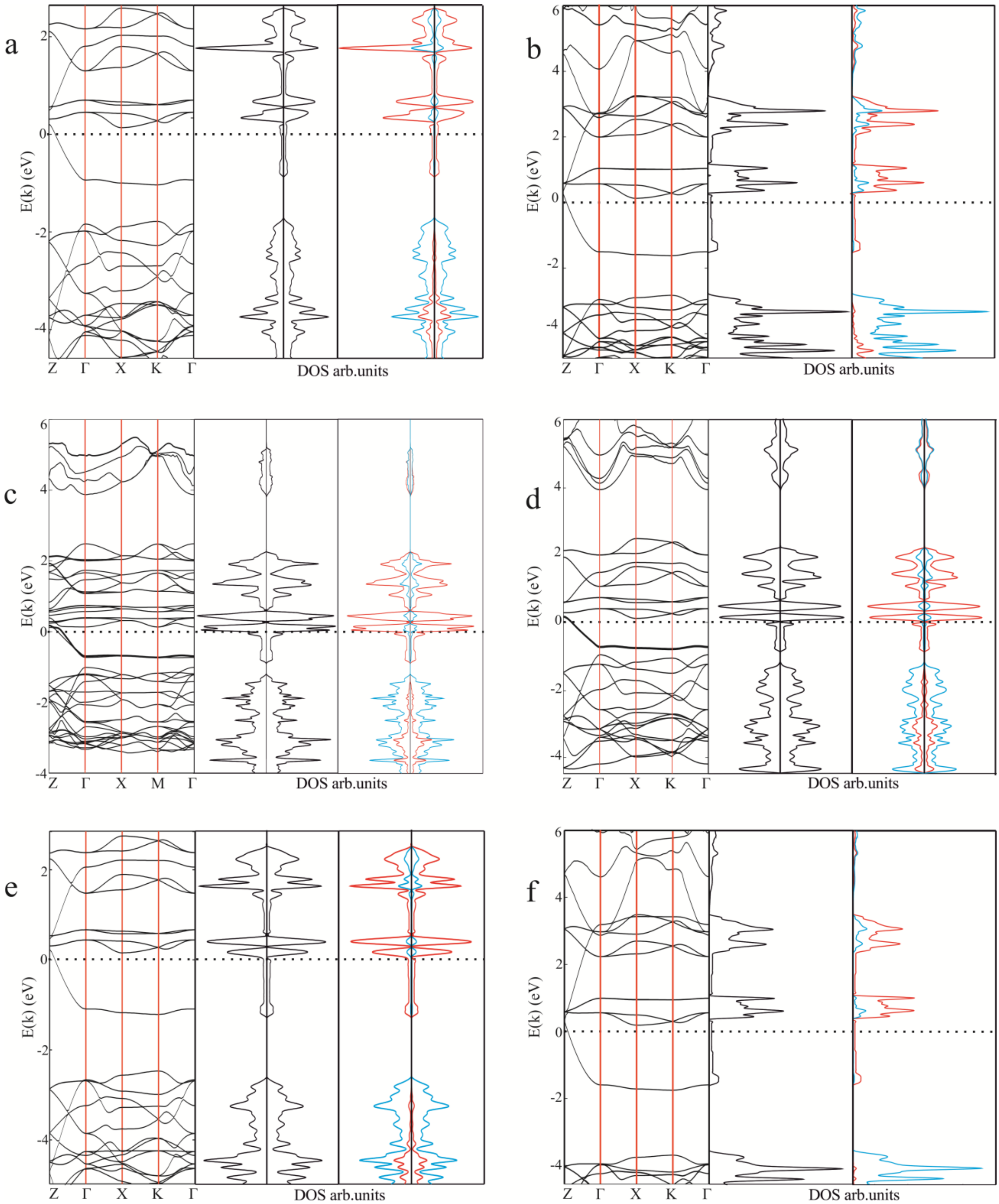

Figure 1S. Band structure, total and partial densities of states for antiferromagnetic ground state of (a) $TiBr_3$, (b) $ZnBr_3$; (c) TiI_3 (hex), (d) TiI_3, (e) $TiCl_3$, (f) $ZrCl_3$. Red and blue lines correspond to the PDOS of metal and halogen atoms, respectively.